Thresholds of Absolute Two-Plasmon–Decay and Stimulated Raman Scattering Instabilities Driven by Multiple Broadband Lasers

R. K. Follett,[1] J. G. Shaw,[1] J. F. Myatt,[2] H. Wen,[1] D. H. Froula,[1] and J. P. Palastro[1]

[1]Laboratory for Laser Energetics, University of Rochester
[2]Department of Electrical and Computer Engineering, University of Alberta

In direct-drive inertial confinement fusion (ICF), a millimeter-scale spherical capsule is illuminated by symmetrically oriented laser beams.[1] The lasers ablate the outer layer of the capsule, which generates pressure to implode the fuel. In addition to depositing thermal energy in the ablator, the lasers can resonantly drive various laser–plasma instabilities that can degrade the quality of the implosion. Large-amplitude electron plasma waves (EPW's) are particularly problematic because they accelerate electrons to suprathermal energies, which can prematurely heat the fuel and impede compression of the capsule. The primary instabilities that generate EPW's in ICF experiments are stimulated Raman scattering (SRS) and two-plasmon decay (TPD).[2]

It has been known since the 1970s that broadband lasers can be used to suppress parametric instabilities,[3,4] but all of the large-scale lasers used in ICF experiments use neodymium glass amplifiers and have very little native bandwidth (<0.1%). There have been a number of studies on parametric instability suppression using excimer gas lasers that have sufficient native bandwidth (~0.1%) to suppress slowly growing instabilities, like filamentation, but not enough to suppress TPD and SRS.[5] Experiments have demonstrated the use of stimulated rotational Raman scattering to significantly increase the bandwidth of both solid-state and gas lasers.[6,7] Another potential path toward high-energy broadband lasers is through the use of optical parametric amplifiers, where a high-energy narrowband laser is used to pump a broadband seed beam. This technique has demonstrated ~70% conversion efficiency to a seed beam with ~5% relative bandwidth at 1053 nm (Ref. 8).

These laser-technology developments have led to a resurgence of interest in using broadband lasers to suppress parametric instabilities in ICF experiments.[9,10] The majority of existing numerical studies considered only one or a few beams in 1-D or 2-D. In actual ICF experiments, many overlapping laser beams are focused onto the target surface. Although the single-beam intensities are typically low, overlapping beams can drive the same plasma waves, resulting in instability even when the intensities of the individual beams are below the single-beam thresholds.[11,12] To assess the viability of using bandwidth to suppress parametric instabilities in ICF experiments, the existing results need to be extended to realistic multibeam geometries.

This summary presents a numerical study of the bandwidth required to suppress absolute TPD and SRS under conditions relevant to direct-drive ICF. Multibeam absolute instability thresholds are obtained for SRS (backscatter and sidescatter) and TPD using 3-D simulations with realistic ICF drive-beam configurations including phase plates and polarization smoothing. Bandwidth is found to be more effective at mitigating multibeam absolute TPD and SRS backscatter than the corresponding single-beam instabilities. The effectiveness of bandwidth at mitigating multibeam absolute SRS sidescatter is found to be similar to the single-beam instability. Despite having the largest fractional increase in threshold relative to the monochromatic case, absolute SRS backscatter has the lowest absolute instability threshold for ignition-relevant plasma conditions over the range of bandwidths considered. Studies of the sensitivity to beam geometry and spectral dispersion suggest that the main results presented here are applicable to a broad range of potential ICF driver geometries.

Figure 1 shows the absolute TPD and SRS thresholds near $n_c/4$ as a function of laser bandwidth for $L_n = 200\ \mu m$, $T_e = 2$ keV [Fig. 1(a)] and $L_n = 400\ \mu m$, $T_e = 4$ keV [Fig. 1(b)]. The thresholds are normalized to the zero-bandwidth thresholds to highlight

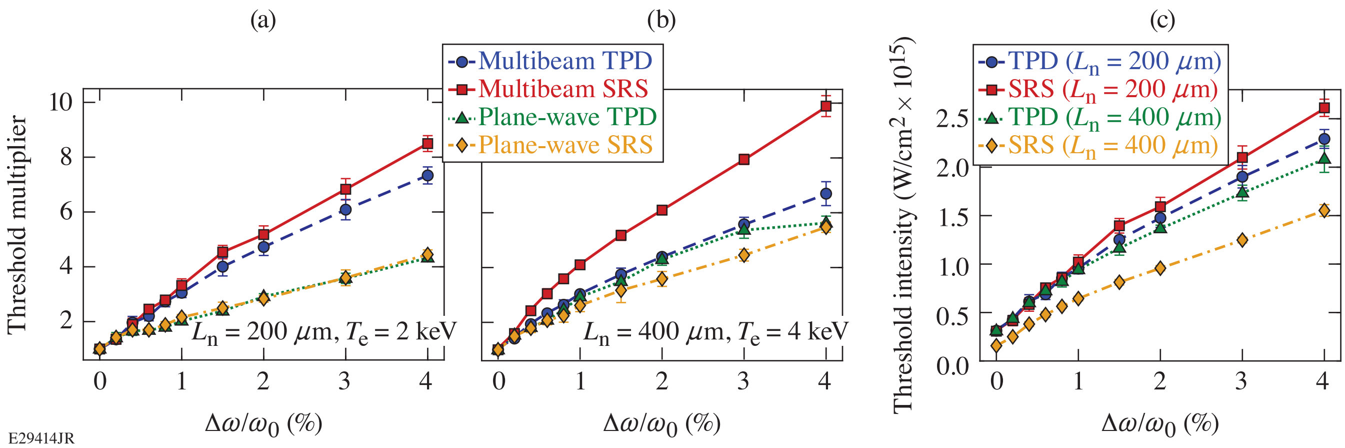

Figure 1
Absolute instability thresholds as a function of the laser normalized to the monochromatic threshold for (a) L_n = 200 μm, T_e = 2 keV and (b) L_n = 400 μm, T_e = 4 keV. The various curves correspond to multibeam TPD (blue circles), multibeam SRS (red squares), single-beam TPD (green triangles), and single-beam SRS (yellow diamonds). (c) The multibeam thresholds from (a),(b) in W/cm^2 for TPD (blue circles) and SRS (red squares) at L_n = 200 μm and TPD (green triangles) and SRS (yellow diamonds) at L_n = 400 μm.

the relative effectiveness of bandwidth mitigation. The error bars correspond to the standard deviation from an ensemble of four threshold calculations with random realizations of polarization, speckle pattern, and spectral phase.

The thresholds for a single plane-wave drive beam are plotted in Figs. 1(a) and 1(b) to show the relative effectiveness of using bandwidth to mitigate single-beam and multibeam instabilities. Intuitively we might expect that the impact of bandwidth on the instability thresholds is independent of the multibeam coupling. If that were the case, the plane-wave and multibeam curves for a given instability would be the same, and only the monochromatic multibeam thresholds and the broadband single-beam thresholds would be needed to calculate the broadband multibeam thresholds. However, the single-beam threshold multipliers are always less than the corresponding multibeam threshold multipliers. This suggests that in addition to increasing the single-beam instability thresholds, broadband lasers reduce the effectiveness of multibeam coupling.

Figure 1(c) shows the multibeam threshold curves from Figs. 1(a) and 1(b) in terms of the absolute overlapped laser intensity (W/cm^2). For the L_n = 200-μm case, the TPD and SRS thresholds are similar at all laser bandwidths. Despite having the largest fractional increase in threshold for a given bandwidth, multibeam SRS with L_n = 400 μm always has the lowest absolute threshold because of its low monochromatic threshold.

This material is based upon work supported by the Department of Energy National Nuclear Security Administration under Award Number DE-NA0003856, ARPA-E BETHE grant number DE-FOA-0002212, the University of Rochester, and the New York State Energy Research and Development Authority.

1. J. Nuckolls *et al.*, Nature **239**, 139 (1972).
2. W. L. Kruer, *The Physics of Laser Plasma Interactions*, Frontiers in Physics, Vol. 73, edited by D. Pines (Addison-Wesley, Redwood City, CA, 1988).
3. J. J. Thomson and J. I. Karush, Phys. Fluids **17**, 1608 (1974).
4. G. Laval *et al.*, Phys. Fluids **20**, 2049 (1977).
5. T. A. Peyser *et al.*, Phys. Fluids B **3**, 1479 (1991).
6. D. Eimerl, D. Milam, and J. Yu, Phys. Rev. Lett. **70**, 2738 (1993).
7. J. Weaver *et al.*, Appl. Opt. **56**, 8618 (2017).
8. C. Dorrer, E. M. Hill, and J. D. Zuegel, Opt. Express **28**, 451 (2020).

9. J. W. Bates *et al*., Phys. Rev. E **97**, 061202(R) (2018).
10. R. K. Follett *et al*., Phys. Plasmas **26**, 062111 (2019).
11. D. F. DuBois, B. Bezzerides, and H. A. Rose, Phys. Fluids B **4**, 241 (1992).
12. C. Stoeckl *et al*., Phys. Rev. Lett. **90**, 235002 (2003).